

Epitaxial growth of $\text{YBa}_2\text{Cu}_3\text{O}_7$ thin films on (100)- SrTiO_3

O. Meyer, F. Weschenfelder, J. Geerk, H. C. Li,* and G. C. Xiong†

Kernforschungszentrum Karlsruhe Institut für Nukleare Festkörperphysik, Postfach 3640, D-7500 Karlsruhe, Federal Republic of Germany

(Received 1 February 1988; revised manuscript received 25 March 1988)

He-ion channeling was applied to analyze the preparation of defect-free (100)- SrTiO_3 surfaces and the growth of large-area single-crystalline $\text{YBa}_2\text{Cu}_3\text{O}_7$ thin films. The analysis supported by Monte Carlo simulation revealed a strain-free growth with the c axis perpendicular to the substrate surface in agreement with reflection high-energy electron diffraction technique measurements. The standard deviation of misoriented regions is 0.2° . The best minimum yield values of 12% are obtained for 1-MeV He ions. Energy-dependent yield measurements show that the films contain dislocations.

The reproducible preparation of high-quality high- T_c oxide superconductors in thin-film form on desired substrates is still a problem of considerable challenge. Most of the deposition techniques use a three-step process: (a) Highly disordered or amorphous material with the stoichiometric composition is deposited at substrate temperatures up to 500°C ; (b) the films are then transformed into the tetragonal phase at about 900°C in 1 atm oxygen (O_2); and (c) the films are finally converted into the orthorhombic high- T_c phase by annealing the tetragonal phase in O_2 at temperatures below 600°C . The phase transformation at 900°C causes considerable interface reactions with various substrates.¹⁻³ Thus, the quality of the films deposited in a three-step procedure with thicknesses below $0.5\ \mu\text{m}$ is rather limited. Furthermore, the nucleation of the crystalline film does not only occur at the film/substrate interface but may occur as well at the surface or at appropriate nucleation centers within the highly disordered film. Therefore, the growth of a large-area single-crystalline high- T_c oxide film is strongly limited.

Recently, a two-step process was developed where the highly crystalline tetragonal phase could successfully be deposited at substrate temperatures of 800°C and below.⁴ Due to these substantially lower substrate temperatures, interface reactions could considerably be suppressed and the quality of the films becomes independent of the film thickness for thicknesses above $0.1\ \mu\text{m}$ and independent of various substrate materials used.

This two-step process has been used to grow high-quality large-area single-crystalline $\text{YBa}_2\text{Cu}_3\text{O}_7$ films on (100) SrTiO_3 . These films show full superconductivity at 89 K with a transition width of 1.2 K. Furthermore, a sharp drop of the Al susceptibility signal is observed at 88 K. The critical current is $1.3 \times 10^6\ \text{A}/\text{cm}^2$ at 77 K in zero magnetic field. Residual resistivity values at 100 K are between 125 and $200\ \mu\Omega\ \text{cm}$ and residual resistivity ratios of about 3 were obtained routinely. As described in the following, the epitaxial growth of these films is analyzed using high-energy ion channeling and reflection high-energy electron diffraction (RHEED). The advantages of ion channeling for interface and epitaxial growth analysis are described in detail elsewhere.⁵ In brief, variations of

compositions at interfaces due to reactions can be analyzed nondestructively together with the crystalline quality of the deposited film as a function of depth. Lattice mismatch and the associated strain can be determined as well as the extent of mosaic spread and the occurrence of special defect structures, e.g., dislocations within the film. In this study, the channeling and backscattering analysis on the as-deposited films has been performed at room temperature using He ions at energies of 1.0, 1.4, and 2.0 MeV and a beam spot of $0.01\ \text{cm}^2$. The beam spot was shifted laterally across the film area in the course of the measurements in order to avoid the accumulation of radiation damage. Monte Carlo calculations have been performed in order to simulate the ion channeling and backscattering process in SrTiO_3 and $\text{YBa}_2\text{Cu}_3\text{O}_7$ single-crystalline films and to analyze the experimental data in more detail.

Previous to deposition, the substrate surface was analyzed by ion channeling and backscattering and the influence of various surface preparation techniques such as polishing, etching, sputtering, and annealing in 1 atm O_2 was studied.

SrTiO_3 single-crystalline substrates obtained from different manufacturers revealed quite different crystalline quality. The minimum yield values χ_{\min} defined as the ratio of the backscattering yields for perfect alignment with the (100) crystal direction to that for random incidence, varied between 1.5% and 30%. The dechanneling yield values were mainly due to high densities of partial dislocations throughout the bulk region. The influence of sputtering and annealing in 1 atm O_2 on the surface peak (SP) of Sr in the (100)-aligned backscattering spectra is demonstrated in Fig. 1. He ions backscattering from Sr and Ti are well separated in energy. The area of the large Sr SP in Fig. 1 (open circles) corresponds to 6.6 Sr atoms per Sr row which was obtained after etching the surface with Ar ions at 400 V and 50 W for 5 min. After annealing at 950°C for 1 h in 1 atm O_2 the SP area (triangles) decreased to 3.0 Sr atoms/Sr row. In order to determine the contribution of thermal vibrations to the yield of the Sr SP, Monte Carlo calculations have been performed using the one-dimensional vibration amplitudes $\langle U_\perp \rangle$ at 300 K of $0.08\ \text{\AA}$ for Sr, $0.062\ \text{\AA}$ for Ti, and an averaged isotro-

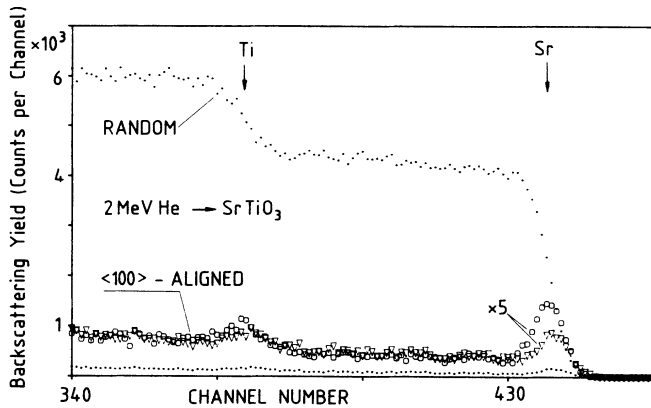


FIG. 1. Random and $\langle 100 \rangle$ -aligned backscattering spectra from SrTiO_3 single-crystalline substrates. The aligned spectra ($\times 5$) are obtained after sputtering the substrate surface with Ar ions (open circles) and after annealing in O_2 (triangles).

pic value of 0.079 \AA for O.⁶ The Sr SP area was calculated to be 3.3 Sr atoms/Sr row for 2-MeV He ions in good agreement with the measured result. The Sr SP area has been analyzed as a function of the incident ion energy between 0.5 and 3.05 MeV and was found to be in good agreement with the calculated values. From these results, it can be concluded that a perfect (100) SrTiO_3 surface can be obtained by ion etching followed by annealing in O_2 . Similar results have been obtained for highly polished and annealed SrTiO_3 surfaces.

Thin films of $\text{YBa}_2\text{Cu}_3\text{O}_7$ were deposited onto well-prepared SrTiO_3 surfaces and were analyzed by ion channeling and backscattering. Monte Carlo simulation calculations have been performed to obtain angular scan curves through the a -, b -, and c -crystal directions in well-defined tilt planes. The one-dimensional vibration amplitudes used were 0.083 \AA for Ba, 0.076 \AA for Y, an averaged value of 0.067 \AA for Cu(1) and Cu(2), and an averaged value of 0.088 \AA for O(1), O(2), O(3), and O(4). These values are all based on high-resolution neutron diffraction measurements.⁷

The best χ_{\min} values of 12% were obtained using 1-MeV

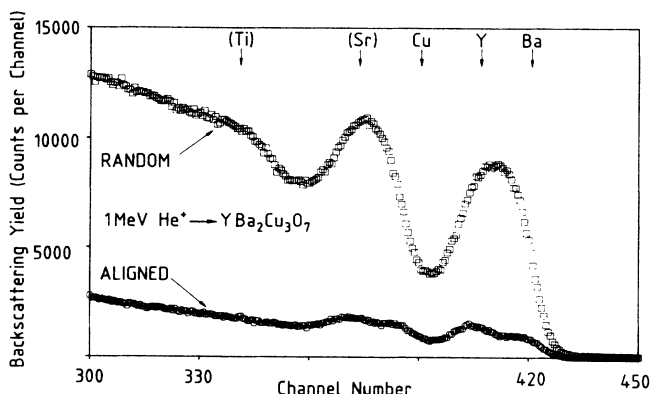


FIG. 2. Random and $\langle 100 \rangle$ -aligned backscattering spectra from an $\text{YBa}_2\text{Cu}_3\text{O}_7$ thin film deposited on (100) SrTiO_3 .

He ions. This is shown in Fig. 2 where the random and $\langle 100 \rangle$ -aligned backscattering spectra are presented. The contributions of the various components in the film and the substrate are indicated by arrows and are resolved to some extent in the aligned spectrum. There is a slight overlap of the Ba yield with the Y yield while both yields are well separated from the Cu yield. The Cu yield, on the other hand, indicates some overlap with the Sr yield from the substrate. The mass separation can be improved by increasing the incident energy E .

In the aligned spectrum of Fig. 2, there is no indication of any mismatch between substrate and film. Such a mismatch would cause an enhanced dechanneling behavior at the interface and deeper in the substrate. A perfect matching between film and substrate further requires a perfect correspondence between the crystal axis and planes of the substrate and the film. Therefore, angular yield curves have been performed throughout the (110), (101), (100), and (010) planes of the substrate and the film and the results are displayed in Fig. 3. The data presented in this figure have been obtained using 2-MeV He ions and energy windows for Ba and Sr as indicated in Fig. 6. The tilt planes were chosen to be perpendicular to the crystal planes. A perfect agreement between the Ba yield and the Sr yield as a function of tilt angle is noted for all major planes, indicating a strain-free growth of the $\text{YBa}_2\text{Cu}_3\text{O}_7$ film on (100) SrTiO_3 .

Further, angular scans through the $\langle 100 \rangle$ crystal direction have been performed and the results are shown in Fig. 4. In addition to the energy windows for Sr and Ba, an energy window for Y is used as indicated in Fig. 6. As the Y yield for the energy and film thickness (60 nm) used is well separated in front of the Sr yield, we could perform reliable angular scan curves for Y as well as for Ba at 2 MeV. The χ_{\min} values for Y, Ba, and Sr are all located at zero tilt angle, again indicating a perfect growth of $\text{YBa}_2\text{Cu}_3\text{O}_7$ on (100) SrTiO_3 . The measured $\psi_{1/2}$ values of 0.90° and 0.88° for Ba and Y are rather close and only slightly smaller than the calculated values of 0.88° and 0.92° for Ba and Y, respectively. The latter difference for

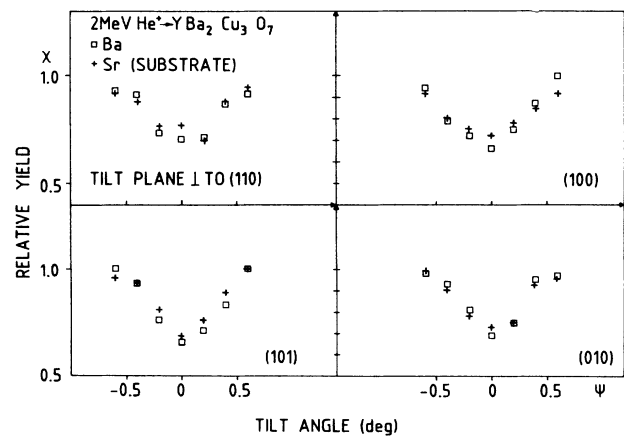


FIG. 3. Angular scans through various crystal planes of the SrTiO_3 substrate and the corresponding planes of the $\text{YBa}_2\text{Cu}_3\text{O}_7$ film.

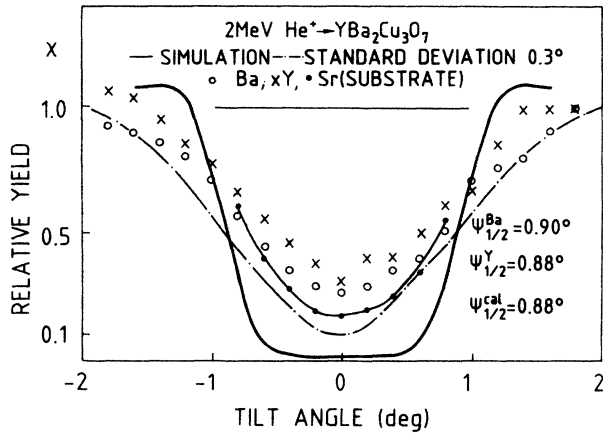


FIG. 4. Angular scans through the $\langle 100 \rangle$ axial direction of $\text{YBa}_2\text{Cu}_3\text{O}_7$ thin film. The angular yield curves for Y, Ba, and Sr (from the substrate) are shown together with a calculated yield curve (solid line) which in turn is convoluted assuming a standard deviation of 0.3° (dashed-dotted line).

Ba and Y in the YBa_2 row along the c direction is due to the different $\langle U_\perp \rangle$ values. In the a or b directions the calculated values are 0.87° and 0.75° for the Ba and Y rows, respectively. The measured and calculated results are compared in Table I. These data clearly show that the c axis of the deposited film is perpendicular to the substrate surface. This result is supported by the RHEED small-angle diffraction pattern given in Fig. 5. The diffraction peaks in c direction are from planes parallel to the substrate surface while the diffraction peaks in $\langle 110 \rangle$ direction are from $\langle 110 \rangle$ planes parallel to the incident electron beam of 14 keV and perpendicular to the substrate surface. The corresponding lattice spacings are $(3a_0)^{-1}$ in c and $(\sqrt{2}a_0)^{-1}$ in the $\langle 110 \rangle$ direction.

The analysis of the angular scan curves and the energy dependence of the aligned spectra (1.0, 1.4, and 2.0 MeV) indicates that at least two kinds of defects are present in the films. First, the product of the dechanneling factor and the defect density is found to increase with \sqrt{E} . This indicates the presence of dislocations.⁵ Second, the shape of the measured angular yield curves being more flat than the calculated one indicates that some regions of the film are slightly misoriented in respect to the substrate. Assuming a Gaussian distribution of the crystallite orientation with a standard deviation of $\sigma = 0.3^\circ$, the slopes and

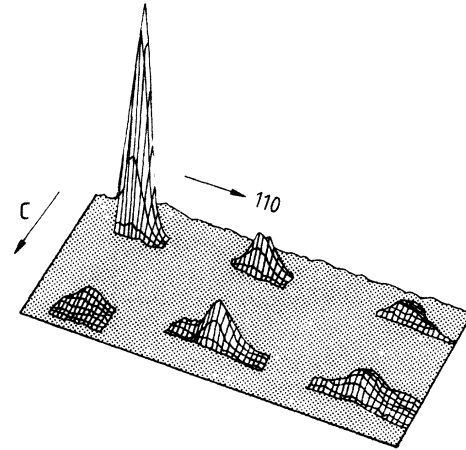


FIG. 5. Small-angle diffraction pattern of a single-crystalline $\text{YBa}_2\text{Cu}_3\text{O}_7$ thin film.

the critical angle of the measured curves can be approximated by the dashed-dotted line in Fig. 4. The remaining parallel shift of this curve with respect to the measured data has to be attributed to the scattering yield from the dislocations. With increasing film thickness up to 600 nm, the best values reached for σ were 0.2° .

Using the ion channeling analysis on the high- T_c oxides, care has to be taken to preserve the nondestructiveness of the method as these materials are extremely sensitive to radiation damage.⁸ This is demonstrated by the channeling and backscattering spectra presented in Fig. 6. The $\langle 100 \rangle$ -aligned spectrum (a) was taken after using a total fluence of $3 \times 10^{15} \text{ He}^+/\text{cm}^2$ at 2 MeV for alignment and measuring spectrum (a). This spectrum has been repeated within an area of about 0.5 cm^2 and was found to be independent of the charge and the sample spot. After increasing the fluence on the same spot by factors of 17 and 34 the spectra b and c , respectively, were obtained. The dechanneling yield of Ba, Y, and Cu is seen to increase by about the same amount, indicating that about the same number of atoms are displaced in the different sublattices. The corresponding displacements-per-atom (DPA) values are 0.002, 0.034, and 0.068, respectively, in good agreement with our previous results where we stated that at about 0.1 DPA the films become x-ray amorphous.⁸

In summary, we have shown by ion channeling and

TABLE I. Measured and calculated values of $\psi_{1/2}$ and χ_{\min} for $\text{YBa}_2\text{Cu}_3\text{O}_7$ single crystals.

Crystal direction	Element	E (MeV)	$\psi_{1/2}^{\text{meas}}$	$\chi_{\min}^{\text{expt}}$	$\psi_{1/2}^{\text{calc}}$	$\chi_{\min}^{\text{calc}}$
c YBa_2 row	Ba	1.0	1.34 ± 0.03	15 ± 4	1.25 ± 0.01	1.5 ± 0.4
	Ba	1.4	1.00 ± 0.03	20 ± 4	1.06 ± 0.01	1.5 ± 0.4
	Ba	2.0	0.90 ± 0.02	25 ± 4	0.89 ± 0.01	1.8 ± 0.4
	Y	2.0	0.88 ± 0.02	25 ± 4	0.92 ± 0.01	1.8 ± 0.4
b	Ba	2.0			0.87 ± 0.01	1.1 ± 0.4
	Y	2.0			0.75 ± 0.01	1.7 ± 0.4

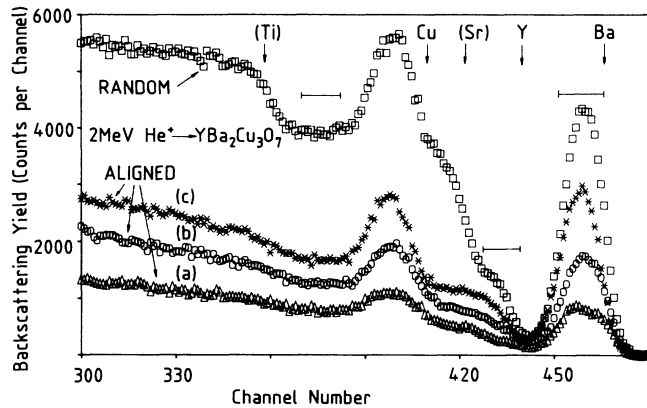


FIG. 6. Random and $\langle 100 \rangle$ -aligned backscattering spectra from an $\text{YBa}_2\text{Cu}_3\text{O}_7$ thin film. The aligned spectra are shown after producing radiation damage with high-energy He ions corresponding to (a) 2×10^{-3} DPA, to (b) 3.4×10^{-2} DPA, and to (c) 6.8×10^{-2} DPA.

backscattering analysis in combination with Monte Carlo calculations that $\langle 100 \rangle$ SrTiO_3 surfaces can be prepared without any distortions.

Onto these surfaces high-quality, large-area (0.5 cm^2) single-crystalline films of $\text{YBa}_2\text{Cu}_3\text{O}_7$ have been produced routinely using an *in situ* two-step process.⁴ The c axis of

these films is perpendicular to the substrate surface. The same growth direction has been observed previously for a certain fraction of the film.⁹ The best minimum yield values of our films were 12% at 1-MeV and 16% at 2-MeV He ions. This is considerably better than values observed previously for films deposited by molecular-beam epitaxy¹⁰ and pulsed laser evaporation.¹¹ It clearly shows that the transformation from the amorphous into the tetragonal phase at about 900°C does not exclusively start at the film/substrate interface. This represents a severe disadvantage of the three-step preparation method.

Although there exists a slight lattice mismatch of 2.1% and 0.5% between the lattice constant of SrTiO_3 and the lattice spacings of the film in the a and b directions, respectively, the interface was found to be free of distortions concerning the composition as well as the lattice strain. This obvious suppression of interface reactions is an important condition for the successful use of other substrate materials. The main damage structures observed for these single-crystalline films were dislocations and a slight mosaic structure ($\sigma = 0.2^\circ$). These defect structures which were observed in all large-area single-crystalline $\text{YBa}_2\text{Cu}_3\text{O}_7$ thin films studied up to now do not seem to affect the superconducting properties to a large extent. Furthermore, we have shown that the films became "channeling" amorphous as well as "x-ray" amorphous at 0.1 DPA due to damage from the incident He^+ beam if it hits too long on one point of the sample.

*On leave from Institute of Physics, Academia Sinica, Beijing, China.

†On leave from Department of Physics, Peking University, China.

¹H. Koinuma, M. Kawasaki, T. Hasimoto, S. Nagata, K. Kitazawa, K. Fueki, K. Masubuchi, and M. Kudo, *Jpn. J. Appl. Phys.* **26**, L763 (1987).

²J. Geerk, H. C. Li, G. Linker, O. Meyer, C. Politis, F. Ratzel, R. Smithey, B. Strehlau, X. X. Xi, and G. C. Xiong, in *Proceedings of the Eighth International Symposium on Plasma Chemistry, Tokyo, 1987*, edited by K. Akashi and A. Kinbara (University of Tokyo, Tokyo, 1987), p. 2349.

³B. Oh, M. Naito, S. Arnason, P. Rosenthal, R. Barton, M. R. Beasley, T. H. Geballe, R. H. Hammond, and A. Kapitulnik, *Appl. Phys. Lett.* **51**, 852 (1987).

⁴H. C. Li, G. Linker, F. Ratzel, R. Smithey, and J. Geerk, *Appl. Phys. Lett.* **52**, 1098 (1988).

⁵L. C. Feldman, J. W. Mayer, and S. T. Picraux, *Materials*

Analysis by Ion Channeling (Academic, New York, 1982).

⁶J. Hutton and R. J. Nelson, *Acta Crystallogr. Sect. A* **37**, 916 (1981).

⁷M. A. Beno, L. Soderholm, D. W. Capone II, D. G. Hinks, J. D. Jorgensen, J. D. Grace, I. K. Schuller, C. U. Serge, and K. Zang, *Appl. Phys. Lett.* **51**, 57 (1987).

⁸B. Egner, J. Geerk, H. C. Li, G. Linker, O. Meyer, and B. Strehlau, in *Proceedings of the Eighteenth International Conference on Low Temperature Physics* [*Jpn. J. Appl. Phys.* **26**, Suppl. 26-3, 2141 (1987)].

⁹P. Chaudhari, R. H. Koch, R. B. Laibowitz, T. R. McGuire, and R. J. Gambino, *Phys. Rev. Lett.* **58**, 2684 (1987).

¹⁰J. Kwo, T. C. Hsieh, R. M. Fleming, M. Hong, S. H. Liou, B. A. Davidson, and L. C. Feldman, *Phys. Rev. B* **36**, 4039 (1987).

¹¹X. D. Wu, D. Dijkkamp, S. B. Ogale, A. Inam, E. W. Chase, P. F. Miceli, C. C. Chang, J. M. Tarascon, and T. Venkatesan, *Appl. Phys. Lett.* **51**, 861 (1987).

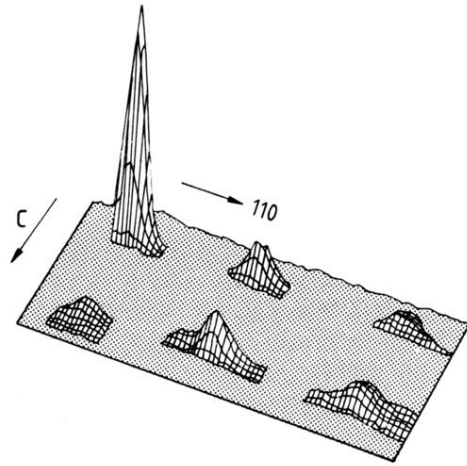


FIG. 5. Small-angle diffraction pattern of a single-crystalline $\text{YBa}_2\text{Cu}_3\text{O}_7$ thin film.